

Discovering Asymptotic Expansions Using Symbolic Regression

Rasul Abdusalamov^{a,*}, Julius Kaplunov^b, Mikhail Itskov^a

^a*Department of Continuum Mechanics, RWTH Aachen University, Germany*

^b*School of Computer Science and Mathematics, Keele University, United Kingdom*

Abstract

Recently, symbolic regression (SR) has demonstrated its efficiency for discovering basic governing relations in physical systems. A major impact can be potentially achieved by coupling symbolic regression with asymptotic methodology. The main advantage of asymptotic approach involves the robust approximation to the sought for solution bringing a clear idea of the effect of problem parameters. However, the analytic derivation of the asymptotic series is often highly nontrivial especially, when the exact solution is not available.

In this paper, we adapt SR methodology to discover asymptotic series. As an illustration we consider three problem in mechanics, including two-mass collision, viscoelastic behavior of a Kelvin-Voigt solid and propagation of Rayleigh-Lamb waves. The training data is generated from the explicit exact solutions of these problems. The obtained SR results are compared to the benchmark asymptotic expansions of the above mentioned exact solutions. Both convergent and divergent asymptotic series are considered. A good agreement between SR expansions and analytical results is observed. It is demonstrated that the proposed approach can be used to identify material parameters, e.g. Poisson's ratio, and has high prospects for utilizing experimental and numerical data.

Keywords: Asymptotic, Symbolic Regression, Kelvin-Voigt Model, Rayleigh-Lamb Waves

1. Introduction

Nowadays with pretense of data, the field of machine learning (ML) gains a major role in scientific research. Recent ML applications range from reducing measurement errors in quantum computations [1] to the acceleration of fluid dynamics simulations [2]. At the same time ML based algorithms have certain disadvantages. In particular, ML suffers from a lack of interpretability, since the algorithms employed are "black box" models. It is often difficult to gain qualitative insights into such models and to fully interpret their behavior. In addition, ML training is usually expensive with respect to computational costs and other resources. Furthermore, biased data may result in inaccurate predictions. Finally, ML algorithms may overfit on a limited data set leading to a poor generalization.

In recent years, symbolic regression (SR) demonstrated substantial potential in addressing some of the above mentioned disadvantages of ML algorithms [3, 4]. The key idea of SR, as described by Augusto et. al. [5], is to establish the structure of an appropriate mathematical model aimed at describing given data. This is achieved by specifying a pool of functions, operations and inputs forming a solution space. The main advantage of this approach is that no a priori assumptions need to be made about the sought for structure of the model. Koza [6] introduced an evolutionary computational technique, known as genetic programming, for searching the solution space. A variety of libraries and frameworks have been developed since then, e.g. see [7] reporting on their performance. At the moment SR is implemented in many areas, including discovering the governing equations for an elastic Timoschenko beam [8], reconstructing orbital anomalies

*Corresponding author

Email address: `abdusalamov@km.rwth-aachen.de` (Rasul Abdusalamov)

[9], accelerating the discovery of novel catalysts [10] as well as investigating dynamic systems [11] just to mention a few.

The implementation of the SR technique may greatly benefit from preliminary physical analysis of the tackled problem, including a definition of problem parameters and scaling laws. This is why the asymptotic analysis has a substantial potential in this field, e.g. see [12]. Asymptotic analysis is a powerful method for simplifying complex relationships to estimate their limiting behavior. It is hardly possible to make here a proper account of the current state of the art in general area of asymptotic methods. Here, we restrict ourselves by mentioning several influential books on the subject, e.g. [13, 14, 15, 16, 17, 18, 19, 20] and references therein. At the same time, asymptotic routines can also get a new powerful impulse from adapting SR. In particular, the calculation of higher order terms may be facilitated in asymptotic expansion even when the exact analytic solution is known but cumbersome. Moreover, SR may be instrumental when the solution is found by a numerical procedure, e.g. using FEM software. In addition, SR appears to be able to extract an asymptotic series from experimental data. Thus, the combination of these two rather different approaches is highly promising for making a substantial impact on the modern research methodology.

In this paper we make an initial effort to apply SR to basics problems in mechanics. Each of them has an explicit exact solution and also allows asymptotic expansions in terms of small or large problem parameters. The exact solutions are used for generating artificial training data to discover SR approximations. However, due to the physical origin of the considered examples, the training data can be equally taken from experimental measurements. The benchmark asymptotic series help to evaluate the accuracy of the obtained SR results.

The paper is organized as follows. Section 2 is concerned with a general introduction into symbolic regression mentioning the prospect for asymptotic series. The simplest example of a two-mass collision problem is considered in Section 3. Despite its simplicity this problem demonstrates three different types of asymptotic behavior. All of them are given by convergent series. An example of a divergent asymptotic series is presented in Section 4, dealing with a viscoelastic Kelvin-Voigt model. Finally, bending wave propagation in an elastic layer is analyzed in Section 5. The previous asymptotic consideration for Rayleigh-Lamb waves, e.g. see [21, 22, 23] are adapted for establishing an SR series. In addition, the obtained SR results are applied for the evaluation of Poisson's ratio. A conclusion and outlook are given in Section 6.

2. Theoretical Background

In the traditional sense, regression is a statistical technique that identifies the relationship between a single dependent variable and one or more independent variables. Typically, an a priori model structure, such as a linear model, is used to determine the best fit for a given set of data. Predefined parameters of the model are optimised. In the case of symbolic regression, no assumptions are made about the model structure or type. SR finds the ideal structure and the relationship between the independent variables and the dependent variable [5]. The result is an algebraic expression that optimally describes the given data set. Typically, such expressions can be described in the form of graphical trees that place operations, constants and inputs in hierarchical relationships (see Figure 1). To find an optimal formulation, most symbolic regression frameworks use genetic programming (GP), an evolutionary computation algorithm. This approach was originally introduced by Koza [6] and utilizes a hierarchical function definition to automatically and dynamically identify potentially candidates. By generating a population of possible solutions and evolving them over a specified number of generations a large search space can be searched in an efficient way. So far SR has been used for a variety of different applications such as material modeling [24, 24, 25, 26] or the discovery of physical relationships [9, 11, 27, 28].

GP algorithms can be split up typically into four different phases: initiation, selection, evolution and termination. In the first phase an initial set of expressions is randomly created from a predefined set of possible mathematical operations, independent variables and functions. This initial set is competing in tournaments during the selection phase. In this way, random subsets are formed and the fittest individual of each subset is determined. In the next phase, the fittest individuals evolve. There are several types of mutations available e.g. *crossover*, *subtree*, *point* or *hoist mutation*. In the case of *crossover* a new individual is formed from a preliminary selected parent and a donor. To this end, a random subtree of the parent is replaced

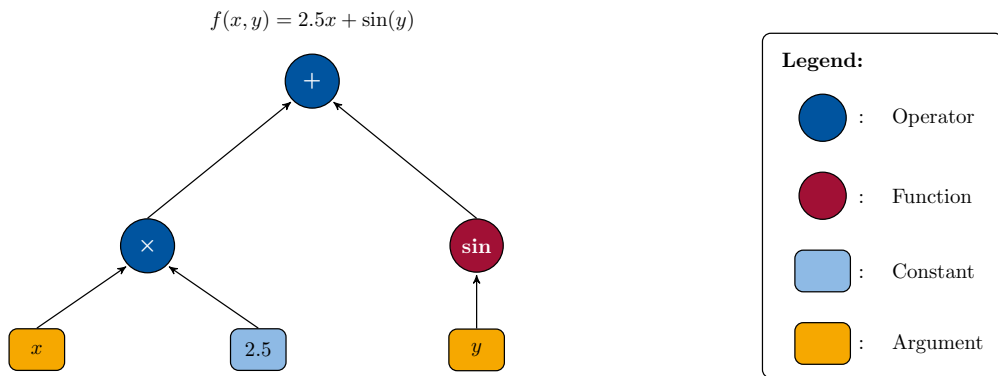


Figure 1: A graphical tree of an algebraic expression.

by a subtree of the donor (see Figure 2). The *subtree mutation* is very similar to *crossover*, however, only

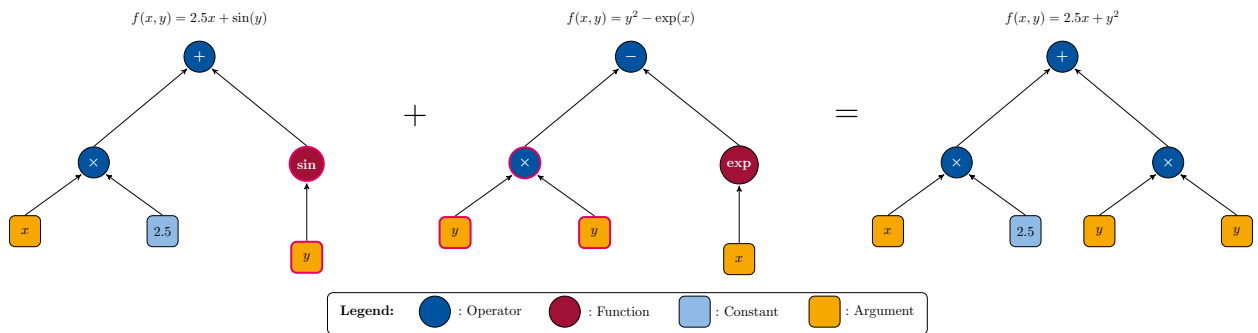


Figure 2: Example of a crossover mutation.

a single parent is needed. In this case, a random subtree is replaced by a random new term allowing to reintroduce forgotten operations, functions or inputs (see for example Figure 3). *Point mutation* is an

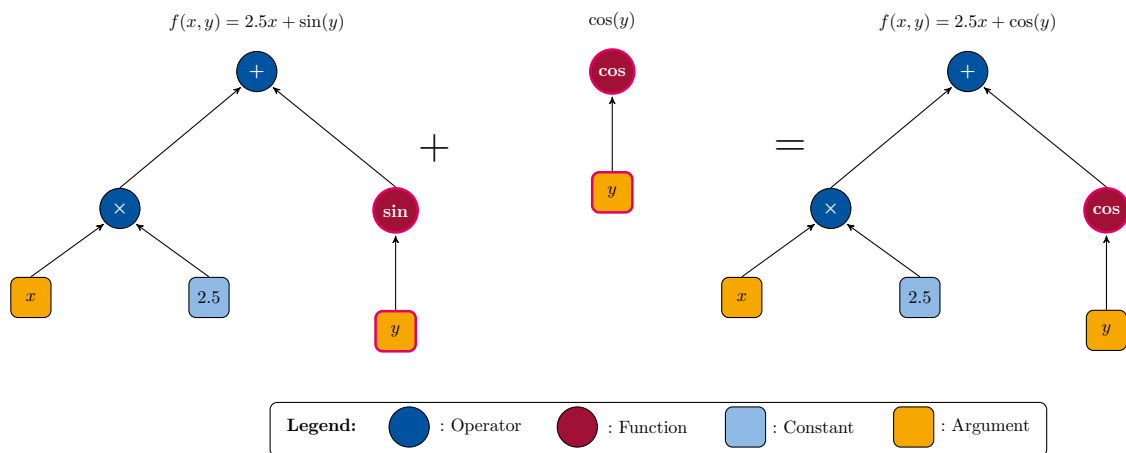


Figure 3: Example of a subtree mutation.

evolution of a single vertex of a tree, see Figure 4. A function, operator or input is replaced with another one. This mutation form also allows to reintroduce lost functions, operations or inputs. The last mutation

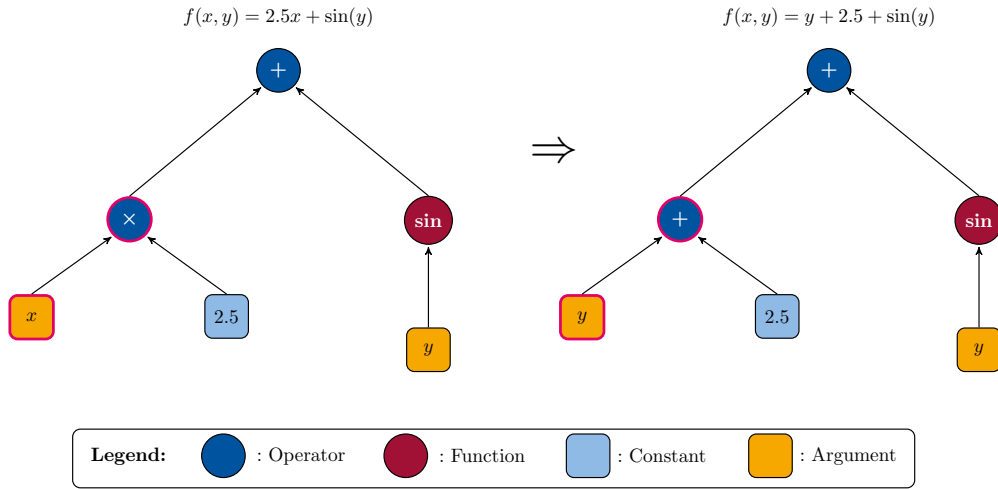


Figure 4: Example of a point mutation.

type called *hoist mutation* is visualized in Figure 5. The goal is to reduce the length of a tree. A random subtree is selected and replaced with a subtree of itself. The selection and evolution process continues until

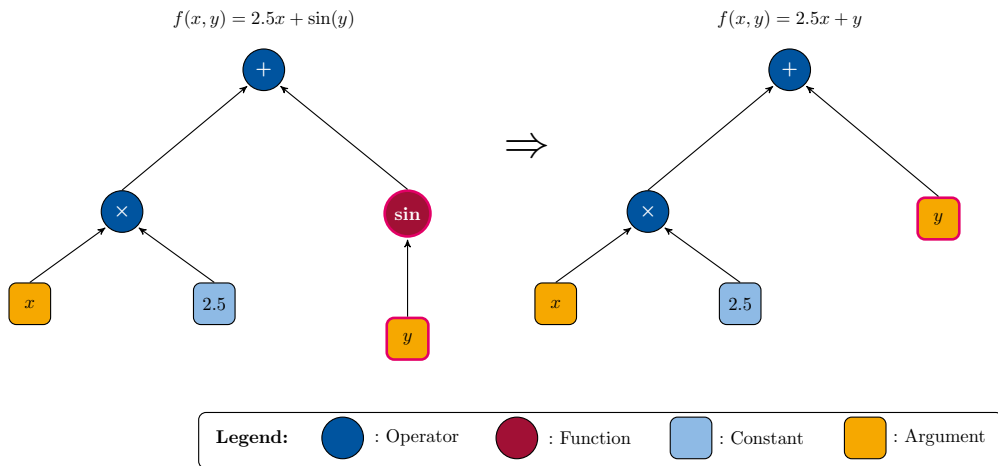


Figure 5: Example of a hoist mutation.

the termination phase. A termination can happen in two ways: either a specified number of generations has been reached or a specified fitness criteria is fulfilled. Note that this procedure does not guarantee to find any optimal solutions. Nevertheless, the overall fitness of the population improves over the number of generations. Additionally, due to the random character of this approach a deterministic solution is not given.

For this work, the Python package `gplearn` is used [29]. For most applications an additional constraint is to restrict the length of the generated expressions. Usually this is done by introducing a Lagrange multiplier as a penalty term into the calculated fitness. To discover asymptotic expansions using symbolic regression, a restriction is counterproductive for developing an asymptotic series. In `gplearn` the parsimony coefficient is responsible to keep the length of the expression small and will have a maximum value of 1×10^{-6} . For the implementation it is necessary to mention that generally symbolic regression has a high sensitivity on hyper parameters. For all examples considered in the following analytical exact solutions are used to generate artificial input data.

Asymptotic analysis is a powerful mathematical technique, often used to simplify complex relations for estimating the limiting behavior of interest e.g. see [12] and references therein . This is usually done by identifying a large/small problem parameter and expanding the sought for solution in term of the series involving this parameter. In the simplest example of a given function $f(\varepsilon)$ that depends on a small parameter ε the asymptotic expansion can be written as

$$f(\varepsilon) = f_0 + f_1\varepsilon + f_2\varepsilon^2 + f_3\varepsilon^3 + \dots,$$

where f_i for $i = 0, 1, 2, \dots$ are the coefficients to be found. In the general case a series of this type can be divergent and its performance strongly depends on the value of the parameter. The evaluation of these coefficients, especially of the higher order ones is often a challenge. The goal of this paper is to adapt an SR approach for determining these coefficients as well as even the powers of the relevant parameter. Moreover, for more general expansions considered in the paper the SR approach is adapted for establishing the basics functions appearing in the asymptotic series.

Below, we present few examples of physically inspired problems originated from mechanics to illustrate the peculiarities of the proposed methodology. The derived SR series are compared with benchmark asymptotic expansions approximating the exact solutions of the studied problems.

3. Collision Problem

In this section we will discuss an illustrative example of the collision of two bodies of mass m_1 and m_2 as shown in Figure 6. For this example, mass m_1 has a prescribed initial velocity v_0 , while mass m_2 is standing still. After the collision, the masses m_1 and m_2 have the velocities v_1 and v_2 , respectively, which are unknown and have to be found. The balance of linear momentum and the balance of kinetic energy are given by

$$m_1 v_0 = m_1 v_1 + m_2 v_2 \quad (1)$$

and

$$\frac{m_1 v_0^2}{2} = \frac{m_1 v_1^2}{2} + \frac{m_2 v_2^2}{2}. \quad (2)$$

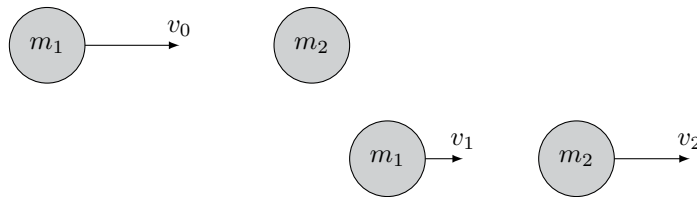


Figure 6: Collision problem for masses m_1 and m_2 (before and after the impact). Here v_0 is the velocity before collision while v_i is the velocity of mass m_i after the collision, $i = 1, 2$.

The solution of these equations is of the form:

$$u_1 = \frac{\delta - 1}{\delta + 1} \quad (3)$$

and

$$u_2 = \delta(1 - u_1), \quad (4)$$

where $\delta = m_1/m_2$ and the dimensionless quantities $u_1 = v_1/v_0$ and $u_2 = v_2/v_0$.

The first of these relations can be expanded into an asymptotic series for three limiting behaviors, including $\delta \gg 1$, $\delta \approx 1$ and $\delta \ll 1$. The strong inequality $\delta \ll 1$ is related to the collision of a mass m_1 with an almost rigid wall. The case $\delta \approx 1$ corresponds to the impulse transfer through masses of almost the same weight. The strong inequality $\delta \gg 1$ governs the collision of a large mass m_1 with a small mass m_2 . The small parameters for each of these three scenarios are $\delta \ll 1$, $\theta = \frac{(\delta-1)}{2} \ll 1$ and $\eta = \frac{1}{\delta} \ll 1$. The associated converging asymptotic series become

$$u_1(\bar{\delta}) = -1 + 2\bar{\delta} - 2\bar{\delta}^2 + 2\bar{\delta}^3 - 2\bar{\delta}^4 + \dots, \quad (5)$$

$$u_1(\theta) = \theta - \theta^2 + \theta^3 - \theta^4 + \dots, \quad (6)$$

and

$$u_1(\eta) = 1 - 2\eta + 2\eta^2 - 2\eta^3 + 2\eta^4 + \dots \quad (7)$$

Now assume that the coefficients as well the powers of the small parameters in the series above are unknown and try to determine both of them using SR. Therefore, data is generated from the exact solution in Equation 3 for the respective domains. To this end, we implement two strategies. The first strategy starts from the chosen small parameter only, i.e. δ , θ or η , specifying it as an input. Alternatively, the inputs can be given in the form of several powers of the small parameter, e.g. for series (5) we can provide the input as $\{\delta, \delta^2, \delta^3\}$. Both strategies were successfully implemented, see Section 6. The discussion below is mainly restricted to the first strategy due to similar outcomes for the two setups in question. Although more inputs are provided for the second strategy, the performance does not necessarily improve.

In Figure 7 we demonstrate the results for only 20 data points specified as the training data for each of limiting setups (5)-(7). The discovered asymptotic expansions with the best fitness are depicted. The convergence of the expansions to the exact solution is shown. The best fits for all three series are listed

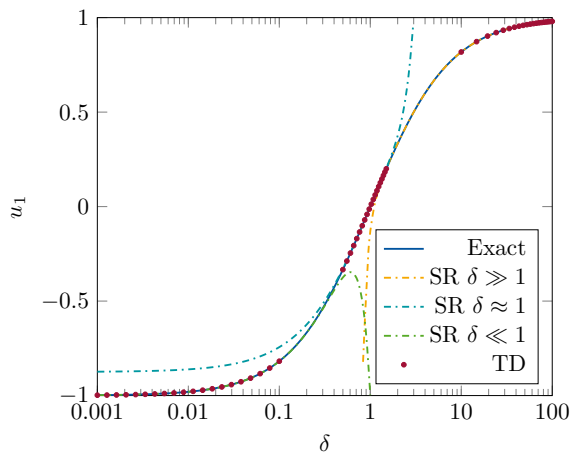


Figure 7: Training data (TD) extracted from exact solution in Equation 3 and SR asymptotic expansions determined for three limiting cases ($\delta \gg 1$, $\delta \approx 1$ and $\delta \ll 1$.)

in Table 1. The randomness of the initial population of the algorithm requires 5 symbolic regressions. In this case, the fitness with respect to the number of generations as well as the best fit of all 5 samples is determined and listed in Tables 4 to 6.

It's worth noting that all automatically constructed asymptotic expansions are close to the exact solution outside a relatively narrow domain, where the training data is given. This is clear from Figure 8, depicting the exact solution, along with its symbolic regression approximation and the training data. Here, only 20 data points calculated by formula (3) are taken. The convergence to the exact solution for $\delta \gg 1$ and $\delta \approx 1$ is illustrated. The sought for coefficients in the determined asymptotic series given above are nearly identical to their exact values up to the 17th order, see Table 1; see also the benchmark coefficients in the expansions (5)-(7).

Table 1: Best SR expansions for all three limiting cases.

Case	Best Approximation	Fitness
$\delta \ll 1$	$u_1(\bar{\delta}) = -1.00 + 2.00\delta - 2.00\delta^2 + 2.00\delta^3 - 2.00\delta^4 + 2.00\delta^5 - 2.00\delta^6 + 2.00\delta^7$ $- 2.00\delta^8 + 2.00\delta^9 - 2.00\delta^{10} + 2.00\delta^{11} - 2.00\delta^{12} + 2.00\delta^{13} - 2.00\delta^{14}$ $+ 2.00\delta^{15} - 2.00\delta^{16} + 2.00\delta^{17}$	5.55×10^{-17}
$\delta \approx 1$	$u_1(\bar{\theta}) = \theta - \theta^2 + \theta^3 - \theta^4 + \theta^5 - \theta^6 + \theta^7 - \theta^8 + \theta^9 - \theta^{10} + \theta^{11} - \theta^{12} + \theta^{13} - \theta^{14}$ $+ \theta^{15} - \theta^{16} + \theta^{17} - \theta^{18} + \theta^{19} - \theta^{20} + \theta^{21} - \theta^{22} + \theta^{23} - \theta^{24} + \theta^{25}$	1.93×10^{-17}
$\delta \gg 1$	$u(\eta) = +1.0 - 2.0\eta + 2.0\eta^2 - 2.0\eta^3 + 2.0\eta^4 - 2.0\eta^5 + 2.0\eta^6 - 2.0\eta^7$ $+ 2.0\eta^8 - 2.0\eta^9 + 2.0\eta^{10} - 2.0\eta^{11} + 2.0\eta^{12} - 2.0\eta^{13} + 2.0\eta^{14}$ $- 2.0\eta^{15} + 2.0\eta^{16} - 2.0\eta^{17}$	3.70×10^{-17}

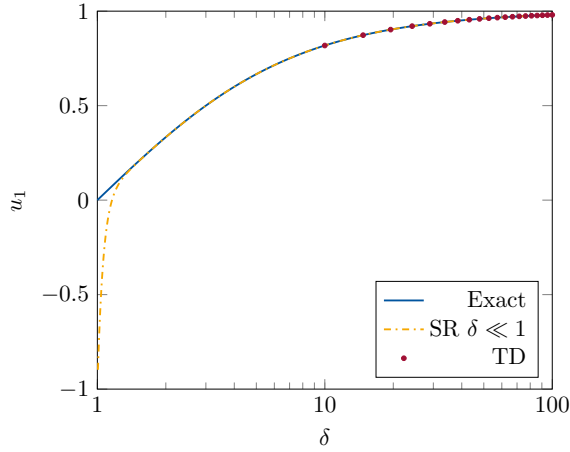


Figure 8: Training data (TD) extracted from exact solution (3) and SR asymptotic series for best approximation (case $\delta \gg 1$), see Table 1.

4. Kelvin-Voigt Viscoelastic Solid

Next consider a more evolved example arising from the viscoelastic Kelvin-Voigt model, e.g. see [30]. Let us start from the constitutive relation (Figure 9)

$$\sigma = E\varepsilon + D \frac{d\varepsilon}{dt}. \quad (8)$$

where σ is the stress, ε is the strain, E is the stiffness of a spring (Young's modulus) and D the viscosity of a damper while t denotes time. This formula can be rewritten in an integral form as

$$\varepsilon(t) = \varepsilon(0) \exp(-\theta t) + \frac{\exp(-\theta t)}{D} \int_{t_1=0}^t \sigma(t_1) \exp(\theta t_1) dt_1,$$

with $\theta = E/D$. Introduce a typical time scale T assuming that $t \gg T$. The limiting large time behavior of the last formula becomes

$$\varepsilon(\tau) = \varepsilon(0) \exp(-\delta \tau) + \frac{T}{D} \exp(-\delta \tau) \int_{\tau_1=0}^{\infty} \sigma(\tau_1) \exp(\delta \tau_1) d\tau_1, \quad (9)$$

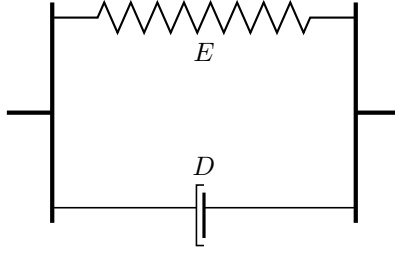


Figure 9: Kelvin-Voigt solid with a spring of stiffness E and a damper of viscosity D .

where $\delta = \theta T$ and $\tau = t/T$.

Next assume that the studied Kelvin-Voigt solid is loaded by the stress depending on time τ as follows

$$\tilde{\sigma}(\tilde{\tau}) = \frac{\sigma_0 \exp((1 - \tilde{\delta})\tilde{\tau})}{1 + \tilde{\delta}\tilde{\tau}},$$

where σ_0 is a prescribed amplitude. In this case, formula (9) can be reduced to

$$\varepsilon(t) = \left(\varepsilon(0) + \frac{T\sigma_0}{D} I(\delta) \right) \exp(-\delta\tau),$$

with (see [31])

$$I(\delta) = \int_0^\infty \frac{\exp(x)}{1 + \tilde{\delta}x} dx = \frac{e^{1/\delta}}{\delta} \Gamma\left(0, \frac{1}{\delta}\right), \quad (10)$$

where Γ denotes the Gamma function.

The integral $I(\delta)$ can be expanded into two different asymptotic series at $\delta \ll 1$ and $\delta \gg 1$. However, in contrast to the previous example the first of them appears to be divergent. The small parameters for each of these scenarios are $\delta \ll 1$ and $\eta = \frac{1}{\delta} \ll 1$. They are given by, e.g. see [32] and references therein,

$$I(\delta) = 1 - \delta + 2\delta^2 - 6\delta^3 + 24\delta^4 + \dots, \quad (11)$$

and

$$I(\eta) = \eta(-\gamma - \log \eta) + \eta^2(1 - \gamma - \log \eta) + \frac{\eta^3}{4}(3 - 2\gamma - 2 \log \eta) + \frac{\eta^4}{36}(11 - 6\gamma - 6 \log \eta) + \dots \quad (12)$$

Therein, γ is the Euler–Mascheroni constant. In this section we adapt the symbolic regression for the construction of the analogs of the series in (11) and (12) using the exact formula for the integral $I(\delta)$ for generating training data. The main focus below is on the effect of the divergent behavior of Equation 11. The numerical results are displayed in Figure 10. Note that for the SR expansions for the case $\eta = \frac{1}{\delta} \ll 1$ the inputs have been provided with $\{\eta, \log \eta\}$.

As expected, in contrast to convergent series, there is a natural threshold for the number of terms in divergent series which can be reproduced with a required accuracy over the chosen domain of the small parameter, see Table 2. The SR higher order terms strongly deviate from their counterparts in benchmarked asymptotic divergent expansions, see also Equations 11 and 12. This is quite obvious, as symbolic regression aims at achieving the best possible accuracy of the provided data, which is not always feasible when using divergent asymptotic series.

The deviation of the benchmark and SR expansions from the exact solution is plotted using the relative root mean square error (RRMSE) in Figure 11 vs. the parameter δ and the highest order n of the retained term in the analyzed series for the case $\delta \ll 1$. In Figure 11 and also in the next Figure 12, the range of the small problem parameter $\tilde{\delta}$ is specified as $2 \times 10^{-4} \leq \delta \leq 0.2$ while $n \leq 8$. It appears that there exists an optimal order n for the analytical divergent series related to the most accurate approximation at the given value of δ . In particular, $n = 4$ in Figure 12 corresponds to $\delta = 0.2$. In this case, however, the accuracy of the SR series is higher approaching a plateau as the order n increases.

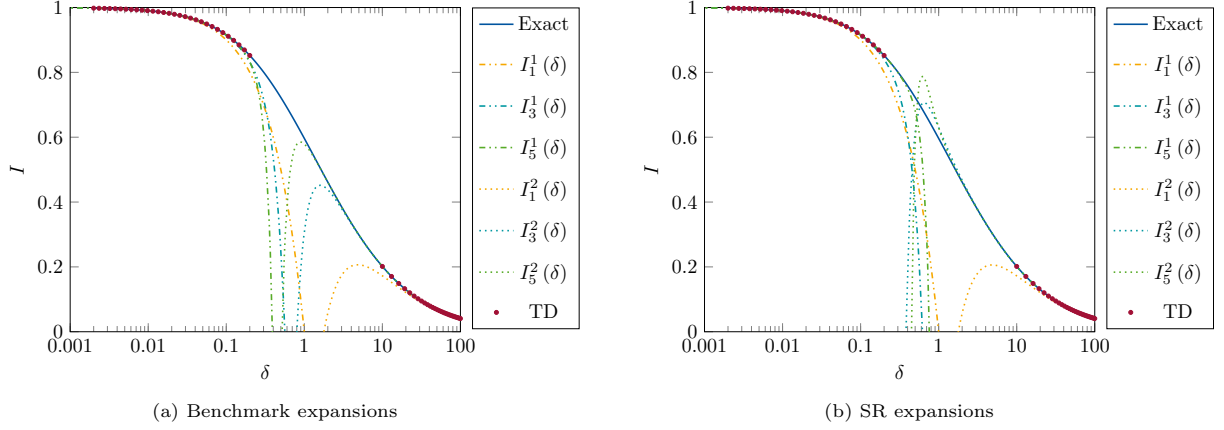


Figure 10: (a) Benchmark and (b) SR asymptotic expansions $I_i^1(\delta)$ and $I_i^2(\tilde{\delta})$ for $\tilde{\delta} \ll 1$ and $\tilde{\delta} \gg 1$, respectively; index i denotes the highest order in Equations 11 and 12.

Table 2: Best SR expansions for all three limiting cases.

Case	Best Approximation	Fitness
$\delta \ll 1$	$I(\delta) = 1.0 - 1.0\delta + 1.95\delta^2 - 4.74\delta^3 + 9.16\delta^4 - 9.12\delta^5 - 1.48\delta^6 + 19.14\delta^7 - 15.34\delta^8$	6.01×10^{-6}
$\delta \gg 1$	$I(\eta) = \eta(-\log \eta - 0.58) + \eta^2(0.42 - 1.0 \log \eta) + \eta^3(0.01 \log \eta^2 - 0.38 \log \eta + 0.79) + \eta^4(-0.06 \log \eta^2 + 0.09 \log \eta) + \eta^5(0.01 \log \eta^3 - 0.03 \log \eta^2 - 0.01 \log \eta) + \eta^6(-0.01 \log \eta^4 - 0.04 \log \eta^3 + 0.02 \log \eta^2) + 0.02\eta^7 \log \eta^2$	2.76×10^{-9}

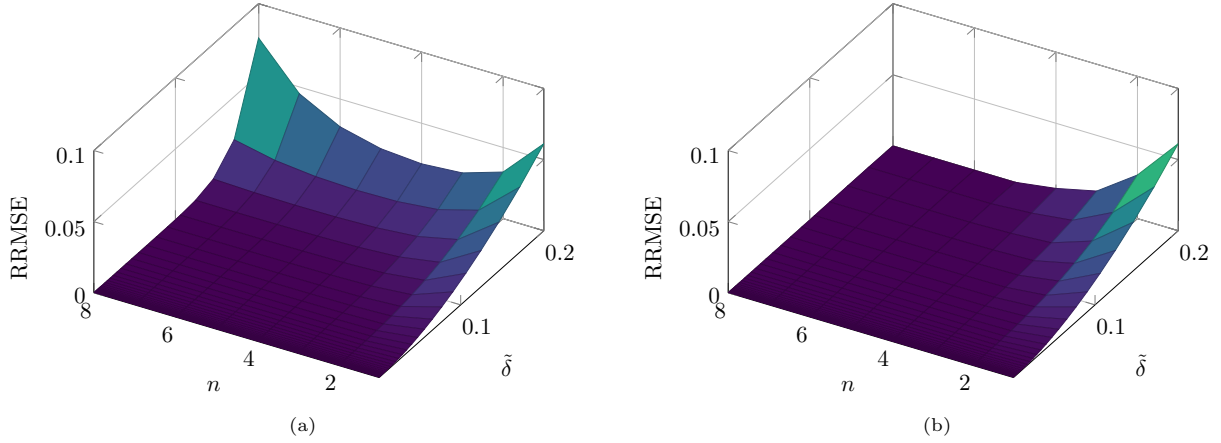


Figure 11: The relative root mean square error (RRMSE) of benchmark and SR expansions, see (11) and (12) as well as Table 2, plotted against exact solution for different orders n and values of δ .

5. Elastic Bending Wave

As the final example, we consider Rayleigh-Lamb waves propagating along an elastic layer of thickness $2h$ with traction free faces (Figure 13), see the original papers [33, 34]. The equation of motion in cartesian

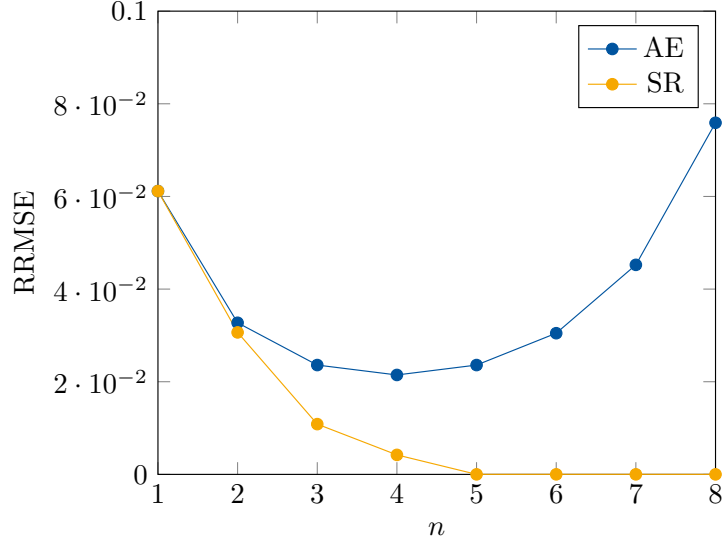


Figure 12: The relative root mean square error (RRMSE) of benchmark analytic expansion (AE) and SR for $\bar{\delta} = 0.2$ plotted against exact solution (10).

coordinates x_1, x_2, x_3 is given by (here and below in this section see [21] for more details)

$$\frac{E}{2(1+\nu)}\Delta\mathbf{u} + \frac{E}{2(1+\nu)(1-2\nu)}\nabla(\nabla\cdot\mathbf{u}) - \rho\frac{\partial^2\mathbf{u}}{\partial t^2} = 0,$$

where E is Young's modulus, ν is Poisson's ratio, ρ the mass density and t time. We restrict ourselves to the plane-strain problem in the plane x_1 - x_3 . In this case, the displacement vector is given by $\mathbf{u} = (u_1, 0, u_3)$. Then the boundary conditions along the faces $x_3 = \pm h$ become

$$\frac{\partial u_3}{\partial x_1} + \frac{\partial u_1}{\partial x_3} = \frac{\nu}{1-\nu}\frac{\partial u_1}{\partial x_1} + \frac{\partial u_3}{\partial x_3} = 0.$$

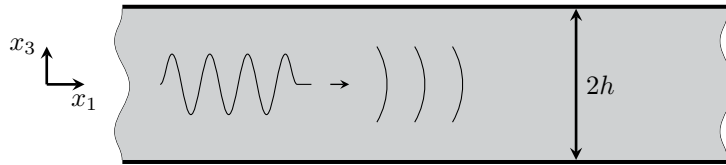


Figure 13: Rayleigh-Lamb waves schematic in an elastic layer.

The associated dispersion relation for antisymmetric traveling waves with angular frequency ω and wavenumber k can be written as

$$\gamma^4 \frac{\sinh \alpha}{\alpha} \cosh \beta - \beta^2 K^2 \cosh \alpha \frac{\sinh \beta}{\beta} = 0, \quad (13)$$

with

$$\gamma^2 = K^2 - \frac{1}{2}\Omega^2, \quad \alpha^2 = K^2 - \kappa^2\Omega^2 \quad \text{and} \quad \beta^2 = K^2 - \Omega^2,$$

where the dimensionless circular frequency $\Omega = \omega h/c_2$, the dimensionless wavenumber $K = kh$, the shear wave speed $c_2 = \sqrt{\frac{E}{2(1+\nu)\rho}}$ and $\kappa = \sqrt{\frac{1-2\nu}{2-2\nu}}$. This equation can be solved numerically, e.g. using a nonlinear

solver in Python. Below the numerical results generated by Python, are used as training data. We also present the low-wave frequency of the fundamental antisymmetric, i.e. bending, mode see also [23, 22], given by

$$K_n^4 = \frac{3}{2}(1 - \nu)\Omega^2 \sum_{j=0}^n A_j \Omega^j, \quad (14)$$

where the first four coefficients A_j take the form

$$\begin{aligned} A_0 &= 1, & A_1 &= \chi \frac{17 - 7\nu}{15(1 - \nu)}, \\ A_2 &= \frac{1179 - 818\nu + 409\nu^2}{2100(1 - \nu)}, & A_3 &= \chi \frac{5951 - 2603\nu + 9953\nu^2 - 4901\nu^3}{126000(1 - \nu)^2}, \end{aligned}$$

with $\chi = \sqrt{3(1-\nu)/2}$.

The best SR approximation is depicted in Figure 14 along with the exact solution and the asymptotic series from formula (14) at the orders $n = 0, 1, 2, 3$. The aforementioned SR approximation has the same coefficients at $n = 3$. Two latter are computed at $\nu = 0.3455$, whereas Poisson's ratio is not specified as an input for the SR approximation. Note that using the determined SR values of the coefficient A_1 or A_2 we may restore the unknown Poisson ratio by the following formulae

$$\nu(A_1) = \frac{119 - 75A_1^2 + 5\sqrt{15}\sqrt{15A_1^4 - 28A_1^2}}{49} \quad (15)$$

or

$$\nu(A_2) = \frac{409 - 1050A_2 + \sqrt{70}\sqrt{15750A_2^2 - 4499}}{409}. \quad (16)$$

This seems promising for the evaluation of Poisson's ratio from experimental data, e.g. see [35, 36]. The convincing results for the considered example are exposed in Table 3.

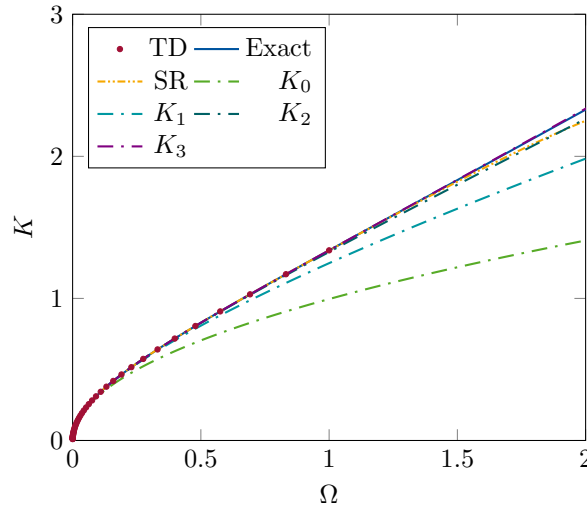


Figure 14: Exact solution of Equation 13 along with its asymptotic expansions K_n^4 by Equation 14 and SR expansion.

Table 3: Determination of Poisson’s ratio from coefficients of SR expansions.

	1	2	3	4	5	Mean	$\nu(A_i)$
A_1	1.48	1.56	1.35	1.59	1.42	1.48	0.36
A_2	0.60	0.57	0.97	0.54	0.81	0.71	0.38

6. Concluding Remarks

In this paper we developed a robust framework to obtain SR asymptotic expansions, illustrated by three problems in mechanics. The proposed methodology was first adapted for an initial simple setup of a two-mass collision problem resulting in the asymptotic expansions expressed through the convergent series corresponding to three limiting behaviors. The SR approximations matched the benchmark analytic expansions up to the 17th order for all mass ratios despite the well-known sensitivity of SR hyperparameters. The example of a Kelvin-Voigt solid is considered to illustrate the peculiarities of SR series for an originally divergent asymptotic expansion. It is observed that the accuracy of an SR expansion makes it superior over the associated optimal analytic series. The last example is concerned with a bending wave propagating along an elastic layer. The long-wave low frequency asymptotic behavior was tackled. A possibility of using the obtained SR results for the evaluation of the unknown Poisson ratio is indicated.

An ”asymptotic” way of thinking is adapted for SR implementation. Although all the training data in this paper are generated using explicit exact solutions, this approach can equivalently be applied to data captured from experiments. Another natural possibility is to make use of numerical data, e.g. FEM simulations. It is remarkable that the obtained SR expansions were discovered from very few data points in comparison with alternative ML techniques. Above we restricted ourselves to basic types of asymptotic behavior. A follow up program may include multi-parametric asymptotic analysis, matched asymptotic expansions as well as Padé approximations and other more involved techniques.

Acknowledgement

Julius Kaplunov gratefully acknowledges the support of the Alexander von Humboldt Foundation which made possible his three months visit to the Department of Continuum Mechanics at RWTH Aachen University in summer 2021.

Appendix

Collision Problem

Table 4: SR expansions for 5 samples ($\delta \ll 1$).

N	Best Approximation	Fitness
1	$u_1(\bar{\delta}) = -1.00 + 2.00\delta - 2.00\delta^2 + 2.00\delta^3 - 2.00\delta^4 + 2.00\delta^5 - 2.00\delta^6 + 2.00\delta^7 - 2.00\delta^8$ $+ 2.00\delta^9 - 2.00\delta^{10} + 2.00\delta^{11} - 2.27\delta^{12} + 4.55\delta^{13} - 4.55\delta^{14} + 4.55\delta^{15} + 9.05\delta^{16}$ $- 9.05\delta^{17} + 36.04\delta^{19}$	2.597×10^{-15}
2	$u_1(\bar{\delta}) = -1.00 + 2.00\delta - 2.00\delta^2 + 2.00\delta^3 - 2.00\delta^4 + 2.00\delta^5 - 2.00\delta^6 + 2.00\delta^7 - 2.00\delta^8$ $+ 2.00\delta^9 - 2.00\delta^{10} + 2.00\delta^{11}$	5.977×10^{-15}
3	$u_1(\bar{\delta}) = -1.00 + 2.00\delta - 2.01\delta^2 + 1.97\delta^3$	5.128×10^{-6}
4	$u_1(\bar{\delta}) = -1.00 + 2.00\delta - 2.00\delta^2 + 2.00\delta^3 - 2.00\delta^4 + 2.00\delta^5 - 2.00\delta^6 + 2.00\delta^7 - 2.00\delta^8$ $+ 2.00\delta^9 - 2.00\delta^{10} + 2.00\delta^{11} - 2.00\delta^{12} + 2.00\delta^{13} - 2.00\delta^{14} + 2.00\delta^{15} - 2.00\delta^{16}$ $+ 2.00\delta^{17}$	5.551×10^{-17}
5	$u_1(\bar{\delta}) = -1.00 + 2.00\delta - 1.99\delta^2 + 1.7137145\delta^3 + 0.01\delta^5 - 0.01\delta^9$	8.108×10^{-7}

Table 5: SR expansions for 5 samples ($\delta \approx 1$).

N	Best Approximation	Fitness
1	$u_1(\bar{\theta}) = \theta - \theta^2 + \theta^3 - \theta^4 + \theta^5 - \theta^6 + \theta^7 - \theta^8 + \theta^9 - \theta^{10} + \theta^{11} - \theta^{12} + \theta^{13} - \theta^{14} + \theta^{15}$ $- \theta^{16} + \theta^{17} - \theta^{18} + \theta^{19} - \theta^{20} + \theta^{21} - \theta^{22}$	1.82×10^{-15}
2	$u_1(\bar{\theta}) = \theta - \theta^2 + \theta^3 - \theta^4 + \theta^5 - \theta^6 + \theta^7 - \theta^8 + \theta^9 - \theta^{10} + \theta^{11} - \theta^{12} + \theta^{13} - \theta^{14} + \theta^{15}$ $- \theta^{16} + \theta^{17} - \theta^{18} + \theta^{19} - \theta^{20} + \theta^{21} - \theta^{22} + \theta^{23}$	1.18×10^{-16}
3	$u_1(\bar{\theta}) = \theta - \theta^2 + \theta^3 - \theta^4 + \theta^5 - \theta^6 + \theta^7 - \theta^8 + \theta^9 - \theta^{10} + \theta^{11} - \theta^{12} + \theta^{13} - \theta^{14} + \theta^{15}$ $- \theta^{16} + \theta^{17} - \theta^{18} + \theta^{19} - \theta^{20} + \theta^{21} - \theta^{22} + \theta^{23}$	4.52×10^{-16}
4	$u_1(\bar{\theta}) = \theta - \theta^2 + \theta^3 - \theta^4 + \theta^5 - \theta^6 + \theta^7 - \theta^8 + \theta^9 - \theta^{10} + \theta^{11} - \theta^{12} + \theta^{13} - \theta^{14} + \theta^{15}$ $- \theta^{16} + \theta^{17} - \theta^{18} + \theta^{19} - \theta^{20} + \theta^{21}$	7.35×10^{-15}
5	$u_1(\bar{\theta}) = \theta - \theta^2 + \theta^3 - \theta^4 + \theta^5 - \theta^6 + \theta^7 - \theta^8 + \theta^9 - \theta^{10} + \theta^{11} - \theta^{12} + \theta^{13} - \theta^{14} + \theta^{15}$ $- \theta^{16} + \theta^{17} - \theta^{18} + \theta^{19} - \theta^{20} + \theta^{21} - \theta^{22} + \theta^{23} - \theta^{24} + \theta^{25}$	1.93×10^{-17}

Table 6: SR expansions for 5 samples ($\delta \gg 1$).

N	Best Approximation	Fitness
1	$u_1(\eta) = 1.0 - 2.0\eta + 2.0\eta^2 - 2.0\eta^3 + 2.0\eta^4 - 2.0\eta^5 + 2.0\eta^6 - 2.0\eta^7 + 2.0\eta^8 - 2.0\eta^9$ $+ 2.0\eta^{10} - 2.0\eta^{11} + 2.0\eta^{12} - 2.0\eta^{13}$	1.23×10^{-17}
2	$u_1(\eta) = + 1.0 - 2.0\eta + 2.0\eta^2 - 2.0\eta^3 + 2.0\eta^4 - 2.0\eta^5 + 2.0\eta^6 - 2.0\eta^7 + 2.0\eta^8 - 2.0\eta^9$ $+ 2.0\eta^{10} - 2.0\eta^{11} + 2.0\eta^{12} - \eta^{13}$	4.68×10^{-15}
3	$u_1(\eta) = + 1.0 - 2.0\eta + 2.0\eta^2 - 2.0\eta^3 + 2.0\eta^4 - 2.0\eta^5 + 2.0\eta^6 - 2.0\eta^7 + 2.0\eta^8 - 2.0\eta^9$ $+ 2.0\eta^{10} - 2.0\eta^{11}$	6.78×10^{-17}
4	$u_1(\eta) = + 1.0 - 2.0\eta + 2.0\eta^2 - 2.0\eta^3 + 2.0\eta^4 - 2.0\eta^5 + 2.0\eta^6 - 2.0\eta^7 + 2.0\eta^8 - 2.0\eta^9$ $+ 2.0\eta^{10} - 2.0\eta^{11} + 2.0\eta^{12} - 2.0\eta^{13} + 2.0\eta^{14} - 2.0\eta^{15} + 2.0\eta^{16} - 2.0\eta^{17}$	3.70×10^{-17}
5	$u_1(\eta) = + 1.0 - 2.0\eta + 2.0\eta^2 - 2.0\eta^3 + 2.0\eta^4 - 2.0\eta^5 + 2.0\eta^6 - 2.0\eta^7 + 2.0\eta^8 - 2.0\eta^9$ $+ 2.0\eta^{10} - 2.0\eta^{11} + 2.0\eta^{12} - 2.0\eta^{13}$	1.02×10^{-15}

Table 7: SR expansions for 5 samples ($\delta \ll 1$) for inputs $\{\delta, \delta^2, \delta^3\}$.

N	Best Approximation	Fitness
1	$u_1(\bar{\delta}) = - 1.0 + 2.0\delta - 2.0\delta^2 + 2.0\delta^3 - 2.0\delta^4 + 2.0\delta^5 - 2.0\delta^6 + 2.0\delta^7 - 2.0\delta^8 + 2.0\delta^9$ $- 2.0\delta^{10} + 2.0\delta^{11} - 1.0\delta^{12} + \delta^{13}$	3.11×10^{-15}
2	$u_1(\bar{\delta}) = - 1.0 + 2.0\delta - 2.0\delta^2 + 2.0\delta^3 - 2.0\delta^4 + 2.0\delta^5 - 2.0\delta^6 + 2.0\delta^7 - 2.0\delta^8 + 2.0\delta^9$ $- 2.0\delta^{10} + 2.0\delta^{11} - 2.0\delta^{12} + 2.0\delta^{13} - 2.0\delta^{14}$	1.48×10^{-16}
3	$u_1(\bar{\delta}) = - 1.0 + 2.0\delta - 2.0\delta^2 + 2.0\delta^3 - 2.0\delta^4 + 2.0\delta^5 - 2.0\delta^6 + 2.0\delta^7 - 2.0\delta^8 + 2.0\delta^9$ $- 2.0\delta^{10} + 2.0\delta^{11} - 2\delta^{12} + 3.0\delta^{13} - 2.0\delta^{14} + \delta^{15} - \delta^{16}$	5.79×10^{-15}
4	$u_1(\bar{\delta}) = - 1.0 + 2.0\delta - 2.0\delta^2 + 2.0\delta^3 - 2.0\delta^4 + 2\delta^5 - 2.0\delta^6 + 2.0\delta^7 - 2.0\delta^8 + 2.0\delta^9$ $- \delta^{10}$	4.25×10^{-14}
5	$u_1(\bar{\delta}) = - 1.0 + 2.0\delta - 2\delta^2 + 2.0\delta^3 - 2.0\delta^4 + 2.0\delta^5 - 2.0\delta^6 + 2.0\delta^7 - 2.0\delta^8 + 2.0\delta^9$ $- 2.28\delta^{10} + 8.85\delta^{11} - 11.85\delta^{12} + 5.28\delta^{13} + 2.0\delta^{14} - 3.0\delta^{15} + \delta^{16}$	4.69×10^{-15}

Table 8: SR expansions for 5 samples ($\delta \approx 1$) for inputs $\{\delta, \delta^2, \delta^3\}$.

N	Best Approximation	Fitness
1	$u_1(\bar{\theta}) = 1.0\theta - 1.0\theta^2 + 1.0\theta^3 - 1.0\theta^4 + 1.0\theta^5 - 1.0\theta^6 + 1.0\theta^7 - 1.0\theta^8 + 1.0\theta^9$ $- 1.0\theta^{10} + 1.0\theta^{11} - 1.0\theta^{12} + 1.0\theta^{13} - 1.0\theta^{14} + 1.0\theta^{15} - 1.0\theta^{16} + 1.0\theta^{17}$ $- 1.0\theta^{18} + 1.0\theta^{19} - 1.0\theta^{20} + 1.0\theta^{21}$	7.344916×10^{-15}
2	$u_1(\bar{\theta}) = \theta - \theta^2 + \theta^3 - \theta^4 + \theta^5 - \theta^6 + \theta^7 - \theta^8 + \theta^9 - \theta^{10} + \theta^{11} - \theta^{12} + \theta^{13} - \theta^{14}$ $+ \theta^{15} - \theta^{16} + \theta^{17}\theta^{18} + \theta^{19} - \theta^{20} + \theta^{21} - \theta^{22}$	7.699281×10^{-16}
3	$u_1(\bar{\theta}) = \theta - \theta^2 + \theta^3 - \theta^4 + \theta^5 - \theta^6 + \theta^7 - \theta^8 + \theta^9 - \theta^{10} + \theta^{11} - \theta^{12} + \theta^{13} - \theta^{14}$ $+ \theta^{15} - \theta^{16} + \theta^{17} - \theta^{18} + \theta^{19} - \theta^{20} + \theta^{21} - \theta^{22} + \theta^{23} - \theta^{24} + \theta^{25}$	3.238150×10^{-17}
4	$u_1(\bar{\theta}) = 1.0\theta - 1.0\theta^2 + 1.0\theta^3 - 1.0\theta^4 + 1.0\theta^5 - 1.0\theta^6 + 1.0\theta^7 - 1.0\theta^8 + 1.0\theta^9 - 1.0\theta^{10}$ $+ 1.0\theta^{11} - 1.0\theta^{12} + 1.0\theta^{13} - 1.0\theta^{14} + 1.0\theta^{15} - 1.0\theta^{16} + 1.0\theta^{17} - 1.0\theta^{18}$	4.876260×10^{-13}
5	$u_1(\bar{\theta}) = \theta - \theta^2 + \theta^3 - \theta^4 + \theta^5 - \theta^6 + \theta^7 - \theta^8 + \theta^9 - \theta^{10} + \theta^{11} - \theta^{12} + \theta^{13} - \theta^{14} + \theta^{15}$ $- \theta^{16} + \theta^{17} - \theta^{18} + \theta^{19} - \theta^{20} + \theta^{21} - \theta^{22} + \theta^{23} - \theta^{24}$	1.159374×10^{-16}

Table 9: SR expansions for 5 samples ($\delta \gg 1$) for inputs $\{\delta, \delta^2, \delta^3\}$.

N	Best Approximation	Fitness
1	$u_1(\bar{\eta}) = 1.0 - 2.00\eta + 1.80\eta^2 + 0.23\eta^3 - 4.71\eta^4 + 1.0\eta^5 - 3.03\eta^6 - 1.0\eta^7 + 6.03\eta^8$ $+ 3.0\eta^9 - 2.0\eta^{10} - 1.0\eta^{12} - 1.00\eta^{13}$	1.73×10^{-5}
2	$u_1(\bar{\eta}) = 1.0 - 2.0\eta + 2.0\eta^2 - 2\eta^3 + 2\eta^4 - 1.87\eta^5 + 0.40\eta^6 + 0.70\eta^7 + 0.89\eta^8$ $+ 1.03\eta^9 + 0.30\eta^{11}$	1.01×10^{-9}
3	$u_1(\bar{\eta}) = 1.0 - 2.0\eta + 2.0\eta^2 - 2.0\eta^3 + 1.98\eta^4 - 1.38\eta^5 - 2.82\eta^6 + 0.62\eta^7 + 1.21\eta^9$ $+ 0.61\eta^{10}$	7.96×10^{-10}
4	$u_1(\bar{\eta}) = 1.0 - 2.0\eta + 2\eta^2 - 2.0\eta^3 + 2.0\eta^4 - 2.0\eta^5 + 2\eta^6 - 2\eta^7 + 2.0\eta^8 - 2.0\eta^9$ $+ \eta^{10} + \eta^{11}$	7.73×10^{-15}
5	$u_1(\bar{\eta}) = 1.0 - 2.0\eta + 2.0\eta^2 - 2.0\eta^3 + 2.0\eta^4 - 2.0\eta^5 + 2.0\eta^6 - 2.0\eta^7 + 2.0\eta^8 - 2.0\eta^9$ $+ 2.0\eta^{10} - 2.0\eta^{11} + 2.0\eta^{12} - 2.0\eta^{13} + 2.0\eta^{14} - 1.0\eta^{15}$	1.17×10^{-16}

Kelvin-Voigt Viscoelastic Solid

Table 10: SR expansions for 5 samples ($\delta \ll 1$).

N	Best Approximation	Fitness
1	$I(\delta) = 1.0 - \delta + 1.86\delta^2 - 3.03\delta^3 - 0.24\delta^4 + 5.97\delta^5 + 5.0\delta^6$	3.23×10^{-5}
2	$I(\delta) = 1.0 - 1.00\delta + 1.78\delta^2 - 2.79\delta^3 - 2.0\delta^4$	4.97×10^{-5}
3	$I(\delta) = 1.0 - \delta + 1.96\delta^2 - 4.42\delta^3 + 3.54\delta^4 + 11.23\delta^5 - 0.27\delta^6 + 0.04\delta^7 + 2.0\delta^8$	8.71×10^{-6}
4	$I(\delta) = 1.0 - 0.943\delta + \delta^2$	5.09×10^{-4}
5	$I(\delta) = 1.0 - 1.0\delta + 1.95\delta^2 - 4.74\delta^3 + 9.16\delta^4 - 9.12\delta^5 - 1.48\delta^6 + 19.14\delta^7 - 15.34\delta^8$	6.01×10^{-6}

Table 11: SR expansions for 5 samples ($\delta \gg 1$).

N	Best Approximation	Fitness
1	$I(\eta) = \eta(-\log \eta - 0.58) + \eta^2(0.45 - \log \eta) + 1.49\eta^3 - 0.38\eta^4 - 0.67\eta^5 + 0.58\eta^6$	2.46×10^{-6}
2	$I(\eta) = \eta(-\log \eta - 0.58) + \eta^2(0.42 - 1.0 \log \eta) + \eta^3(0.01 \log \eta^2 - 0.38 \log \eta + 0.79)$ $+ \eta^4(-0.06 \log \eta^2 + 0.09 \log \eta) + \eta^5(0.01 \log \eta^3 - 0.03 \log \eta^2 - 0.01 \log \eta)$ $+ \eta^6(-0.01 \log \eta^4 - 0.04 \log \eta^3 + 0.02 \log \eta^2) + 0.02\eta^7 \log \eta^2$	2.76×10^{-9}
3	$I(\eta) = \eta(-\log \eta - 0.58) + \eta^2(0.42 - \log \eta) + \eta^3(0.36 - 0.53 \log \eta) + 0.94\eta^4$	1.91×10^{-7}
4	$I(\eta) = \eta(-1.0 \log \eta - 0.58) + \eta^2(1 - \log \eta) + \eta^3(0.43 \log \eta^3 - 0.25 \log \eta^2 - 2.22 \log \eta)$ $+ \eta^4(0.17 \log \eta^4 + 1.65 \log \eta^3 - 2.79 \log \eta^2 - 3.21 \log \eta)$ $+ \eta^5(-0.17 \log \eta^5 + 0.54 \log \eta^4 + 1.91 \log \eta^3 - 5.64 \log \eta^2 + 0.21 \log \eta)$ $+ \eta^6(-1.02 \log \eta^5 - 0.56 \log \eta^4 + 2.02 \log \eta^3 + 0.57 \log \eta^2 + 1.34 \log \eta)$ $+ \eta^7(-1.88 \log \eta^5 - 2.2 \log \eta^4 + 3.6 \log \eta^3 - 0.44 \log \eta)$ $+ \eta^8(-1.0 \log \eta^5 - 0.17 \log \eta^4 + 4.13 \log \eta^3 - 5.24 \log \eta^2 + 1.0 \log \eta)$ $+ \eta^9(0.61 \log \eta^3 + 4.41 \log \eta^2 + 3.29 \log \eta) + \eta^{10}(1.0 \log \eta^3 + 0.9 \log \eta^2 - 2.58 \log \eta)$	1.97×10^{-5}

N	Best Approximation	Fitness
5	$ \begin{aligned} I(\eta) = & -0.87\eta \log \eta + \eta^2 \log \eta^2 (0.02 \log \eta^3 - 0.04 \log \eta^1 + 0.02) \\ & + \eta^3 \log \eta (0.03 \log \eta^5 + 0.12 \log \eta^4 - 0.01 \log \eta^3 - 0.3 \log \eta^2 + 0.19 \log \eta^1 - 0.04) \\ & + \eta^4 \log \eta (0.01 \log \eta^6 + 0.01 \log \eta^5 + 0.11 \log \eta^4 + 0.03 \log \eta^3 - 0.51 \log \eta^2) \\ & + \eta^4 \log \eta (0.48 \log \eta^1 - 0.14) + \eta^5 \log \eta (-0.02 \log \eta^8 + 0.01 \log \eta^7 + 0.10 \log \eta^6) \\ & + \eta^5 \log \eta (+0.03 \log \eta^5 + 0.34 \log \eta^4 + 0.2 \log \eta^3 - 1.59 \log \eta^2 + 1.15 \log \eta^1 - 0.21) \\ & + \eta^6 (-0.54 \log \eta^5 + 1.16 \log \eta^4 - 1.95 \log \eta^3 + 1.83 \log \eta^2 - 0.61 \log \eta) \\ & + \eta^6 (-0.01 \log \eta^{10} - 0.06 \log \eta^9 + 0.01 \log \eta^8 + 0.37 \log \eta^7 - 0.19 \log \eta^6) \\ & + \eta^7 (-2.52 \log \eta^5 + 3.56 \log \eta^4 - 2.89 \log \eta^3 + 1.76 \log \eta^2 - 0.30 \log \eta) \\ & + \eta^7 (-0.03 \log \eta^{10} - 0.19 \log \eta^9 + 0.05 \log \eta^8 + 1.18 \log \eta^7 - 0.62 \log \eta^6) \\ & + \eta^8 (-0.06 \log \eta^{10} - 0.42 \log \eta^9 - 0.06 \log \eta^8 + 2.79 \log \eta^7 - 0.90 \log \eta^6) \\ & + \eta^8 (-6.74 \log \eta^5 + 9.32 \log \eta^4 - 5.06 \log \eta^3 + 1.6 \log \eta^2 - 0.46 \log \eta) \\ & + \eta^9 (-0.09 \log \eta^{10} - 0.66 \log \eta^9 - 0.28 \log \eta^8 + 4.8 \log \eta^7 - 0.80 \log \eta^6) \\ & + \eta^9 (-13.55 \log \eta^5 + 18.17 \log \eta^4 - 9.65 \log \eta^3 + 2.24 \log \eta^2 - 0.17 \log \eta) \\ & + \eta^{10} (-0.11 \log \eta^{10} - 0.89 \log \eta^9 - 0.52 \log \eta^8 + 6.85 \log \eta^7 - 0.30 \log \eta^6) \\ & + \eta^{10} (-21.87 \log \eta^5 + 28.7 \log \eta^4 - 14.81 \log \eta^3 + 3.14 \log \eta^2 - 0.2 \log \eta) \\ & + \eta^{11} (-27.65 \log \eta^5 + 34.6 \log \eta^4 - 17.26 \log \eta^3 + 3.22 \log \eta^2 - 0.07 \log \eta) \\ & + \eta^{11} (-0.05 \log \eta^{10} - 0.75 \log \eta^9 - 1.1 \log \eta^8 + 6.92 \log \eta^7 + 2.15 \log \eta^6) \\ & + \eta^{12} (-0.25 \log \eta^9 - 0.88 \log \eta^8 + 3.95 \log \eta^7 + 3.64 \log \eta^6 - 24.62 \log \eta^5) \\ & + \eta^{12} (30.5 \log \eta^4 - 14.11 \log \eta^3 + 1.4 \log \eta^2 + 0.36 \log \eta) \\ & + \eta^{13} (-0.19 \log \eta^8 + 1.28 \log \eta^7 + 2.47 \log \eta^6 - 14.48 \log \eta^5) \\ & + \eta^{13} (18.14 \log \eta^4 - 7.53 \log \eta^3 - 0.19 \log \eta^2 + 0.49 \log \eta) \\ & + \eta^{14} (0.27 \log \eta^7 + 0.7598 \log \eta^6 - 4.87 \log \eta^5 + 6.86 \log \eta^4 - 2.98 \log \eta^3) \\ & + \eta^{14} (-0.56 \log \eta^2 + 0.51 \log \eta) + \eta^{15} (0.03 \log \eta^6 - 0.66 \log \eta^5) \\ & + \eta^{15} (1.51 \log \eta^4 - 0.8701 \log \eta^3 - 0.29 \log \eta^2 + 0.29 \log \eta) \\ & + \eta^{16} (-0.04 \log \eta^5 + 0.09 \log \eta^4 - 0.05 \log \eta^3 - 0.02 \log \eta^2 + 0.02 \log \eta) \end{aligned} $	4.74×10^{-6}

Elastic Bending Wave

Table 12: SR expansions for 5 samples.

N	Best Approximation	Fitness
1	$K^4 = -0.01\Omega + 1.01\Omega^2 + 1.45\Omega^3 + 0.6\Omega^4 + 0.16\Omega^5$	2.14×10^{-4}
2	$K^4 = 0.97\Omega^2 + 1.53\Omega^3 + 0.57\Omega^4 + 0.07\Omega^5 + 0.08\Omega^6 + 0.03\Omega^7 - 0.03\Omega^8 - 0.03\Omega^9 - 0.01\Omega^{10} + 0.01\Omega^{11} + 0.01\Omega^{12}$	4.71×10^{-5}
3	$K^4 = 1.0\Omega^2 + 1.33\Omega^3 + 0.97\Omega^4 - 0.21\Omega^5 + 0.12\Omega^6$	1.97×10^{-5}
4	$K^4 = 0.95\Omega^2 + 1.56\Omega^3 + 0.54\Omega^4 + 0.15\Omega^5 + 0.03\Omega^6 - 0.02\Omega^7$	7.53×10^{-5}
5	$K^4 = 0.99\Omega^2 + 1.39\Omega^3 + 0.81\Omega^4 - 0.03\Omega^5 + 0.05\Omega^6$	3.6707×10^{-5}

References

- [1] A. Seif, K. A. Landsman, N. M. Linke, C. Figgatt, C. Monroe, M. Hafezi, Machine learning assisted readout of trapped-ion qubits, *Journal of Physics B: Atomic, Molecular and Optical Physics* 51 (2018) 174006.
- [2] D. Kochkov, J. A. Smith, A. Alieva, Q. Wang, M. P. Brenner, S. Hoyer, Machine learning-accelerated computational fluid dynamics, *Proceedings of the National Academy of Sciences* 118 (2021) e2101784118.
- [3] P. Orzechowski, W. La Cava, J. H. Moore, Where are we now? a large benchmark study of recent symbolic regression methods, in: *Proceedings of the Genetic and Evolutionary Computation Conference, GECCO '18, Association for Computing Machinery, New York, NY, USA, 2018*, p. 1183–1190.
- [4] Y. Wang, N. Wagner, J. M. Rondinelli, Symbolic regression in materials science, *MRS Communications* 9 (2019) 793–805.
- [5] D. Augusto, H. Barbosa, Symbolic regression via genetic programming, in: *Proceedings. Vol.1. Sixth Brazilian Symposium on Neural Networks, 2000*, pp. 173–178.
- [6] J. R. Koza, Genetic programming as a means for programming computers by natural selection, *Statistics and computing* 4 (1994) 87–112.
- [7] W. La Cava, P. Orzechowski, B. Burlacu, F. O. de França, M. Virgolin, Y. Jin, M. Kommenda, J. H. Moore, Contemporary symbolic regression methods and their relative performance, *arXiv preprint arXiv:2107.14351*.
- [8] Z. Huang, C. Li, Z. Huang, Y. Wang, H. Jiang, AI-Timoshenko: Automatedly Discovering Simplified Governing Equations for Applied Mechanics Problems From Simulated Data, *Journal of Applied Mechanics* 88, 101006.
- [9] M. Manzi, M. Vasile, Orbital anomaly reconstruction using deep symbolic regression, *71st International Astronautical Congress*.
- [10] B. Weng, Z. Song, R. Zhu, Q. Yan, Q. Sun, C. G. Grice, Y. Yan, W.-J. Yin, Simple descriptor derived from symbolic regression accelerating the discovery of new perovskite catalysts, *Nature communications* 11 (2020) 1–8.
- [11] S. Gaucel, M. Keijzer, E. Lutton, A. Tonda, Learning dynamical systems using standard symbolic regression, *European Conference on Genetic Programming (2014)* 25–36.
- [12] I. V. Andrianov, L. I. Manevitch, *Asymptotology: ideas, methods, and applications*, Vol. 551, Springer Science & Business Media, 2002.
- [13] C. M. Bender, S. A. Orszag, *Advanced mathematical methods for scientists and engineers I: Asymptotic methods and perturbation theory*, Vol. 1, Springer Science & Business Media, 1999.
- [14] J. Kevorkian, J. D. Cole, *Perturbation methods in applied mathematics*, Vol. 34, Springer Science & Business Media, 2013.
- [15] M. V. Fedoryuk (Ed.), *Partial differential equations V: Asymptotic methods for partial differential equations*, Springer, Berlin, Heidelberg, 1999.
- [16] A. Naife, *Introduction to perturbation methods*, M.: Mir.
- [17] E. T. Copson, E. T. Copson, *Asymptotic expansions*, Cambridge university press, 2004.
- [18] N. G. De Bruijn, *Asymptotic methods in analysis*, Vol. 4, Courier Corporation, 1981.
- [19] J. G. Simmonds, J. E. Mann Jr, *A first look at perturbation theory*, Courier Corporation, 1998.
- [20] S. M. Bauer, S. B. Filippov, A. L. Smirnov, P. E. Tovstik, R. Vaillancourt, *Asymptotic methods in mechanics of solids*, Vol. 167, Springer, 2015.
- [21] J. D. Kaplunov, L. Y. Kossovitch, E. Nolde, *Dynamics of thin walled elastic bodies*, Academic Press, 1998.
- [22] A. Gol'denveyzer, Y. D. Kaplunov, E. Nol'de, Asymptotic analysis and refinements of the theories of plates and shells of timoshenko-reissner type, *Izv. Ross. Akad. Nauk. Mekh. Tverd. Tela* (1990) 124–138.

- [23] A. Goldenveizer, J. Kaplunov, E. Nolde, On timoshenko-reissner type theories of plates and shells, *International Journal of Solids and Structures* 30 (1993) 675–694.
- [24] E. Kablman, A. H. Kolody, M. Kommenda, G. Kronberger, Prediction of stress-strain curves for aluminium alloys using symbolic regression, in: *AIP Conference Proceedings*, Vol. 2113, AIP Publishing LLC, 2019, p. 180009.
- [25] G. Bomarito, T. Townsend, K. Stewart, K. Esham, J. Emery, J. Hochhalter, Development of interpretable, data-driven plasticity models with symbolic regression, *Computers & Structures* 252 (2021) 106557.
- [26] R. Abdusalamov, M. Hillgärtner, M. Itskov, Automatic generation of interpretable hyperelastic material models by symbolic regression, *International Journal for Numerical Methods in Engineering* 124 (2023) 2093–2104. doi:<https://doi.org/10.1002/nme.7203>.
URL <https://onlinelibrary.wiley.com/doi/abs/10.1002/nme.7203>
- [27] Z. Huang, C. Li, Z. Huang, Y. Wang, H. Jiang, Ai-timoshenko: Automatedly discovering simplified governing equations for applied mechanics problems from simulated data, *Journal of Applied Mechanics* 88.
- [28] S. Sun, R. Ouyang, B. Zhang, T.-Y. Zhang, Data-driven discovery of formulas by symbolic regression, *MRS Bulletin* 44 (2019) 559–564.
- [29] T. Stephens, Gplearn (2015), URL <https://gplearn.readthedocs.io/en/stable/index.html>.
- [30] R. Christensen, *Theory of viscoelasticity: an introduction*, Elsevier, 2012.
- [31] A. Prudnikov, Y. A. Brychkov, O. I. Marichev, *Integrals and series, volume 1: Elementary functions*, Gordon&Breach Sci. Publ., New York.
- [32] A. Erdélyi, *Asymptotic expansions*, Courier Corporation, 1956.
- [33] H. Lamb, On waves in an elastic plate, *Proceedings of the Royal Society of London. Series A, Containing papers of a mathematical and physical character* 93 (1917) 114–128.
- [34] L. Rayleigh, On the free vibrations of an infinite plate of homogeneous isotropic elastic matter, *Proceedings of the London Mathematical Society* 1 (1888) 225–237.
- [35] J. Kaplunov, E. Nolde, N. Veksler, Determination of parameters of elastic layer by measured dispersion curves of zero-order lamb-type waves, *Proceedings of the Estonian Academy of Sciences. Physics. Mathematics*.
- [36] W. P. Rogers, Elastic property measurement using rayleigh-lamb waves, *Research in Nondestructive Evaluation* 6 (1995) 185–208.